Non-linear vibrations of an idealized saccular aneurysm

C. Ramón-Lozano[1], D. Aranda-Iglesia[1], J. A. Rodríguez-Martínez[1]

[1] Department of Continuum Mechanics and Structural Analysis, University Carlos III of Madrid, Leganés, Spain,
clara.ramon@alumnos.uc3m.es, faranda@ing.uc3m.es, jarmarti@ing.uc3m.es

Abstract

Intracranial saccular aneurysms are a small portion of a vessel that bulges outward forming a balloon like sac. Approximately 3% of the worldwide population suffer from this pathology and its rupture entails subarachnoid haemorrhage, causing in most of the cases brain damage or even death. Many physical and clinical factors highly affect their evolution; however, the main criteria for deciding their treatment is size.

The main contribution of this work is to develop a 3D mathematical model to describe the behaviour of an idealized intracranial saccular aneurysm. A study of its mechanical behaviour is performed to understand under which conditions the aneurysm will break. It is studied under three situations: subjected to an internal constant pressure and surrounded by a non-viscous Newtonian fluid, subjected to an internal constant pressure and surrounded by a viscous Newtonian fluid and subjected to an internal pulsatile pressure and surrounded by a viscous Newtonian fluid. Then, some parameters as the total pressure or the thickness of the wall are varied to understand how they influence their rupture.

1. Introduction

According to Tortora and Derrickson [1], an aneurysm is "a thin, weakened section of the wall of an artery or a vein that bulges outward, forming a balloonlike sac". They are classified in three main groups: aortic, peripheral and cerebral. Among the last one, saccular aneurysms are the most common cerebral aneurysms and seem to be the most common cause of non-traumatic subarachnoid haemorrhage [2-3].

In order to understand the rupture of saccular aneurysms, it is important to study their mechanical behaviour. Some researches as Akkas [4] and Austin et al. [5] signalled that aneurysm's rupture was derived from the apparition of limit point instabilities in the quasi-static response. In contrast, some other authors as Jain [6], Sekhar and Heros [7] and Sekhar et al. [8] proposed that rupture appeared when the pulsatile blood flow excited the natural frequency of the aneurysm's wall, making it dynamically instable. This hypothesis was also supported by Simkins and Stehbens [9] and Hung and Botwin [10] but it was soon discarded since all these authors were assuming the shell membrane theory, which assumes infinitesimal strains and linear material behaviour. Additionally, they were not considering a surrounding cerebrospinal fluid (CSF).

Later, Shah and Humphrey [11] and David and Humphrey [12] introduced an internal pulsatile pressure and the pressure given by the CSF. Moreover, they studied the elastodynamics using a Fung-type pseudostrain-energy function, concluding that these parameters were responsible of an increase in the stability of aneurysm's wall. Furthermore, comparing the effect of different constitutive models they conclude that for a correct understanding of the dynamic behaviour of these structures, the strain-energy function has to be specifically calibrated for biological tissues to avoid non-real instabilities.

However, those authors developed their model in a 2-D framework and others as MacDonald et al. [13] and Costalat et al. [14] demonstrated that shell-membrane theory is not valid for all aneurysm's thicknesses since radial stresses play an important role in this type of lesions. Therefore, due to the necessity of developing a 3D framework to describe the dynamic behaviour of previous researches, this paper extends the work of Humphrey and co-workers [11-12] considering a surrounding CSF and two different constitutive models. Additionally, we perform a parametric analysis to analyse which biological parameters influence into the rupture of these aneurysms.

2. Problem Formulation

In this section, we extend the work of Humphrey et al. [11-12] and we develop a 3D mathematical model of the problem of an intracranial saccular aneurysm surrounded by the CSF.

2.1. The Aneurysm's Wall

In the framework of non-linear finite elasticity, the aneurysm's wall is considered isotropic and incompressible. In spherical coordinates (R, Θ, Φ), the aneurysm occupies a volume Ω_0 in a reference configuration where $A \leq R \leq B$, being A the inner radius and B the outer one. Following the work of Costalat et al. [14] the values for the inner and outer radius correspond with $A = 4.3$ mm and $B = 4.67$ mm. The wall is deformed in such a manner that it maintains the spherical symmetry, being the motion in spherical polar coordinates (r, θ, ϕ) in a Ω configuration where $r(R, t)$ and $a \leq r \leq b$, being a and b the inner and outer deformed radius respectively.

So, setting the equilibrium for an infinitesimal spherical volume element, the balance of linear momentum in the radial direction is

$$\frac{\partial \sigma_r}{\partial r} + 2 \frac{(\sigma_r - \sigma_\theta)}{r} = \rho \ddot{r} \qquad (1)$$

where superimposed dots mean differentiation with respect to time, $\sigma_r(r, t)$ and $\sigma_\theta(r, t)$ the radial and

circumferential Cauchy stresses and $\rho = 1050$ kg/m^3 the density of the aneurysm's wall [11].

Since the radial and circumferential stretches are $\lambda_r = \frac{\partial r}{\partial R}$ and $\lambda_\theta = \lambda_\phi = \lambda = \frac{r}{R}$, assuming the incompressibility condition ($\lambda_r \lambda_\phi \lambda_\theta = 1$) it is deduced that

$$\lambda(r,t) = \left(\frac{B^3}{R^3}\left(\lambda_b^3 - 1\right) + 1\right)^{\frac{1}{3}} \qquad (2)$$

where $\lambda_b = \frac{b}{B}$ is the circumferential stretch in the outer wall of the aneurysm. Then, by calculating the derivatives of equation (2) with respect to r and t

$$\frac{\partial \lambda}{\partial r} = -\frac{\lambda^3 - 1}{R} \qquad (3)$$

$$\ddot{\lambda} = \frac{\lambda^3 - 1}{\lambda_b^3 - 1}\left(\frac{2\lambda_b \dot{\lambda}_b^2 + \lambda_b^2 \ddot{\lambda}_b}{\lambda^2} - \frac{2\lambda_b^4 \dot{\lambda}_b^2}{\lambda^5}\frac{\lambda^3 - 1}{\lambda_b^3 - 1}\right) \qquad (4)$$

where superimposed dots mean derivation of the λ with respect to time. Then, by introducing eq. (3) and eq. (4) into eq. (1), the balance of linear momentum results as

$$\frac{\partial \sigma_r}{\partial \lambda} - 2\frac{(\sigma_r - \sigma_\theta)}{\lambda(\lambda^3 - 1)} =$$

$$= \rho B^2 \left(\frac{2\lambda_b^4 \dot{\lambda}_b^2}{(\lambda_b^3 - 1)^{\frac{4}{3}}}\frac{(\lambda^3 - 1)^{\frac{1}{3}}}{\lambda^5} - \frac{2\lambda_b \dot{\lambda}_b^2 + \lambda_b^2 \ddot{\lambda}_b}{(\lambda_b^3 - 1)^{\frac{1}{3}}}\frac{1}{\lambda^2(\lambda^3 - 1)^{\frac{2}{3}}}\right) \qquad (5)$$

From the work of Ogden et al. [15] it is known that for an incompressible shell $\sigma_r - \sigma_\theta = -\frac{1}{2}\lambda\frac{d\psi}{d\lambda}(\lambda^{-2}, \lambda, \lambda)$, being ψ the strain-energy function, which describes the mechanical behaviour of the material. Introducing the previous relation and integrating eq. (5) over the thickness of the aneurysm, we obtain that

$$P_b(t) - P_a(t) + \int_{\left(\frac{\lambda_b^3 + f_0 - 1}{\lambda_b}\right)^{\frac{1}{3}}}^{\lambda_b} \frac{\psi'(\lambda)}{\lambda^3 - 1}d\lambda = \rho B^2 \left(\lambda_b \ddot{\lambda}_b\left(\frac{\lambda_b}{(\lambda_b^3 + f_0 - 1)^{\frac{1}{3}}} - 1\right)\right) -$$

$$-\rho B^2 \left(\dot{\lambda}_b^2 \left(\frac{\lambda_b^4}{2(\lambda_b^3 + f_0 - 1)^{\frac{4}{3}}} - \frac{2\lambda_b}{(\lambda_b^3 + f_0 - 1)^{\frac{1}{3}}} + \frac{3}{2}\right)\right) \qquad (6)$$

where prime ($'$) denotes differentiation with respect the circumferential stretch. Moreover, the dimensionless parameter $f_0 = \frac{A^3}{B^3} = 0.78$ characterizes the thickness of the aneurysm's wall and $P_a(t)$ and $P_b(t)$ describe the blood pressure and the pressure exerted by the CSF on the aneurysm respectively.

2.2. Blood Pressure

The aneurysm's wall is subjected to two different internal pressures. Eq. (7a) shows a constant blood pressure and eq. (7b) a pulsatile radially symmetric blood pressure, based on the data measured by Ferguson [16] for saccular aneurysms and assuming the pressure is uniform inside.

$$P_a = P_m \qquad (7a)$$

$$P_a(t) = P_m + \sum_{n=1}^{N}(A_n\cos(n\omega t) + B_n\sin(n\omega t)) \qquad (7b)$$

$P_m = 65.7$ mmHg is the mean pressure and A_n and B_n are the Fourier coefficients for N harmonics, being ω the fundamental circular frequency. According to the work by Shah and Humphrey [11], we use five harmonics that are: $A_1 = -7.13$, $B_1 = 4.64$, $A_2 = -3.08$, $B_2 = -1.18$, $A_3 = -0.13$, $B_3 = 0.564$, $A_4 = -0.205$, $B_4 - 0.346$, $A_5 = 0.0662$ and $B_5 = -0.12$, all in mmHg.

2.3. Cerebrospinal Fluid

The aneurysm is surrounded by the CSF. Considering it to be incompressible and Newtonian, it is described by

$$P_b(t) = -p_\infty - \rho_f B^2\left(\frac{3}{2}\dot{\lambda}_b^2 - \lambda_b\ddot{\lambda}_b\right) - 4\mu\frac{\dot{\lambda}_b}{\lambda_b} \qquad (8)$$

where ρ_f and μ are the density and viscosity of the CSF respectively.

2.4. Non-linear Governing Equation

Finally, by introducing the pressure expressions into eq. (6), and making all non-dimensional, the non-linear governing equation arises:

$$\overline{\Delta P} = \int_{\lambda_b}^{\left(\frac{\lambda_b^3 + f_0 - 1}{\lambda_b}\right)^{\frac{1}{3}}} \frac{\overline{\psi}'(\lambda)}{\lambda^3 - 1}d\lambda + 4\kappa\frac{\dot{\lambda}_b}{\lambda_b} - \overline{\rho}\left(\lambda_b\ddot{\lambda}_b + \frac{3}{2}\dot{\lambda}_b^2\right) -$$

$$\lambda_b\ddot{\lambda}_b\left(1 - \frac{\lambda_b}{(\lambda_b^3 + f_0 - 1)^{\frac{1}{3}}}\right) - \dot{\lambda}_b^2\left(\frac{\lambda_b^4}{2(\lambda_b^3 + f_0 - 1)^{\frac{4}{3}}} - \frac{2\lambda_b}{(\lambda_b^3 + f_0 - 1)^{\frac{1}{3}}} + \frac{3}{2}\right) \qquad (9)$$

where now, superimposed dots denote differentiation with respect the dimensionless time. This equation returns some dimensionless groups such the dimensionless pressure $\overline{\Delta P} = \frac{P_a(t)}{C_{N10}} - \frac{P_\infty}{C_{N10}}$, the dimensionless strain-energy function $\overline{\psi}(\lambda) = \frac{\psi(\lambda)}{C_{N10}}$ and the dimensionless harmonics $\overline{A_i} = \frac{A_i}{C_{N10}}$ and $\overline{B_i} = \frac{B_i}{C_{N10}}$, all non-dimensionalized with the parameter C_{N10}, which is a parameter empirically determined for the aneurysm's wall. Other groups as $\kappa = \frac{\mu}{B\sqrt{\rho C_{N10}}}$ defines the ration between the characteristics time scales (speed of stress waves) of CSF and aneurysm's wall, $\overline{\rho}$ the ratio between the CSF and aneurysm's wall densities and $\overline{\omega} = \omega\sqrt{\frac{\rho B^2}{C_{N10}}}$ the dimensionless fundamental angular frequency.

2.5. Constitutive Model

In this work, we employ two different strain-energy functions corresponding to the Neo-Hookean and the 3-parameters Mooney-Rivlin models to describe the mechanical behaviour of the aneurysm's wall.

- Neo-Hookean Model

$$\psi = C_{N10}(I_1 - 3) \qquad (10)$$

- 3-parameters Mooney-Rivlin Model

$$\psi = C_{M10}(I_1 - 3) + C_{M01}(I_2 - 3) + C_{M11}(I_1 - 3)(I_2 - 3) \qquad (11)$$

I_1 and I_2 are the first two invariants of the left Cauchy-Green deformation tensor. According to data obtained by Costalat et al. [14] using experimental results obtained from 16 intracranial saccular aneurysms tested in uniaxial tension under physiological conditions, $C_{M10} = 0.19$ MPa, $C_{M01} = 0.024$ MPa and $C_{M11} = 7.87$ MPa. For the

Neo-Hookean model, $C_{N10} = 0.214$MPa has been selected to ensure that Neo-Hookean and Mooney-Rivlin models provide the same initial shear modulus. A comparison between these models is performed to disclose the role of the mechanical behaviour of the wall into the dynamic response of the aneurysm.

2.6. Numerical Solution

Eq. (9) can be reduced to a system of two first-order differential equations. Being $z_1 = \lambda_b$ and $z_2 = \dot{\lambda}_b$:

$$z_2 = \dot{z}_1$$

$$\dot{z}_2 = \frac{\overline{\Delta P} - \int_{z_1}^{\left(\frac{\lambda_b^3 + f_0 - 1}{\lambda_b}\right)^{\frac{1}{3}}} \frac{\psi'(\lambda)}{\lambda^3 - 1} d\lambda - 4\kappa \frac{z_2}{z_1} + z_2^2\left(\frac{3}{2} + \frac{z_1^4}{2(z_1^3 + f_0 - 1)^{\frac{4}{3}}} - \frac{2z_1}{(z_1^3 + f_0 - 1)^{\frac{1}{3}}} - \frac{3}{2}\overline{\rho}\right)}{z_1\left(\overline{\rho} + \frac{z_1}{(z_1^3 + f_0 - 1)^{\frac{1}{3}}} - 1\right)} \quad (12)$$

This system of differential equations is solved numerically using a fourth-order Runge-Kutta method available in MATLAB for stiff differential equations. Recall that the motion of every material point along the aneurysm's wall is determined once λ_b is known.

For a detailed derivation of the problem formulation, see the final bachelor thesis named "Non-linear vibrations of an idealized saccular aneurysm" [17].

3. Results

As presented before, in this work we analyse how different biological parameters affect the dynamic stability of an idealized saccular aneurysm. Consequently, we present how it behaves when it is subjected to a constant internal pressure and non-viscous CSF, to a viscous CSF and finally, to an internal variable pressure. The reference values employed in this analysis are taken from the works of Shah and Humphrey [11] and Costalat et al. [14] and correspond with: $\rho = 1050$ kg/m³, $\rho_f = 1000$ kg/m3, $p_\infty = 3$ mmHg and $A = 4.3$ mm and $B = 4.67$ mm. In the graphs, the reference case is marked with an asterisk.

During the parametric analysis, we look for the bifurcation point (the point at which the wall of the aneurysm stops oscillating) and then analyse if the value reached by the parameter we are varying is biologically achievable or not. In all the cases, we also see that whereas for the Neo-Hookean model we reach a bifurcation, we never achieve one for the case of Mooney-Rivlin. This occurs because since the order of the Mooney-Rivlin model is higher that the framework of the formulation, the model will never bifurcate. By this way, since the Mooney-Rivlin is of O(4) and the mathematical formulation of O(3), a bifurcation never occurs no matter the value of the parameter we are varying. Consequently, we see that the mathematical formulation is highly dependent in the constitutive model we choose.

3.1. Non-viscous CSF and Constant Blood Pressure

For the most basic case we have varied the dimensionless value of pressure. As seen in figure 1a, the phase diagram shows that the aneurysm is oscillating until we reach a value of $\overline{\Delta P} = 0.185$, where a bifurcation occurs in the
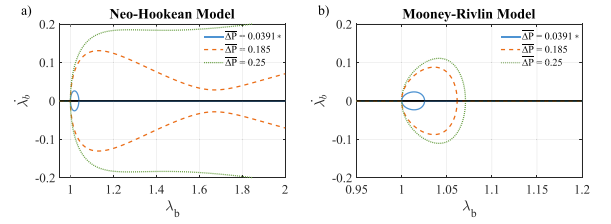

Figure 1: *Comparison of the aneurysm's model for Neo-Hookean and Mooney-Rivlin model. For various $\overline{\Delta P}$ at $f_0 = 0.7806$, $\overline{\rho} = 0.9524$ and $\kappa = 0$.*
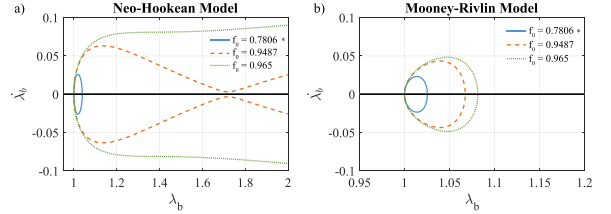

Figure 2: *Comparison of the aneurysm's model for Neo-Hookean and Mooney-Rivlin model for various f_0 at $\overline{\Delta P} = 0.0391$, $\overline{\rho} = 0.9524$ and $\kappa = 0$.*

case of Neo-Hook. However, this value is not biologically achievable since, according to the data provided by Williams et al. [18], adults with severe hypertension will achieve values of pressure equal or higher to 180 mmHg, which corresponds with a dimensionless pressure of 0.1121. Nevertheless, even though this value is not high enough for the bifurcation to occur and is relatively far from the pressure needed (about 296 mmHg) it seems that the influence of pressure is relevant enough and it should be explored for other and more accurate constitutive models. Graph 1b shows the behaviour of the aneurysm's wall for the Mooney-Rivlin. As expected, no bifurcation occurs although significantly high values as $\overline{\Delta P} = 1000$ has been tried. Hence, we see that the behaviour of the aneurysm's model highly depends in the constitutive model we select.

Now, continuing with figure 2, the variations with respect to the internal and external radius are explored. As before, three different situations appear, one with the reference case and another two exploring the bifurcations points. So, for the case of Neo-Hookean model, the bifurcations appear at a value of $f_0 = 0.9478$. In constrast with the previous case, there exits a limit thickness for which a bifurcation occurs and consequently, the rupture of the aneurysm. We know from literature that the thickness of aneurysms vary considerably, finding small aneurysms with a thickness between 0.02 mm and 0.08 mm, whose models can be calculated assuming the membrane's theory, and others with larger thickness as 0.375mm or even 0.51mm. Consequently, those aneurysims with a thickness around 0.08 mm or smaller [19], whose $f_0 \sim 0.92590$ or higher will break.

3.2. Viscous CSF and Constant Blood Pressure

In a first attempt, the model has been computed with the viscosity given by Shat et al. [11]. $\mu = 1.26 \cdot 10^{-4}$ Ns/m², which corresponds with a value of $\kappa = 1.8 \cdot 10^{-6}$. However we see that for this value the behaviour of the aneurysm experiments no change and that the
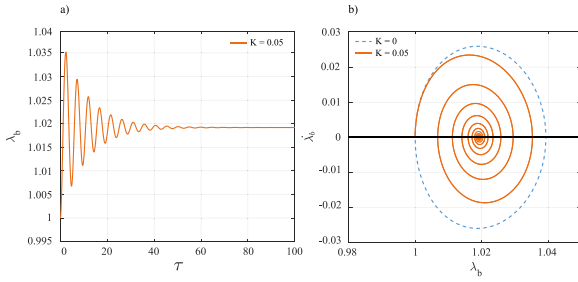
Figure 3: *Aneurysm's model at reference conditions ($\Delta P = 0.0391$, $\overline{\rho} = 0.9524$ and $f_0 = 0.7806$) with a viscosity of $\kappa = 0.05$ and a constant internal pressure for the Neo-Hookean model. Graph a) shows how the stretch evolves over time and graph b), the phase diagram.*

viscosity value required for the oscillation to attenuate is far from the achievable ones. However, since the parameter κ is influenced by other parameters as the external radius, the density of the solid or the constitutive model parameter, we explore in figure 3 the point at which the model will experiment an attenuation of the oscillation. From graph 3a and 3b it can be easily deduced that the aneurysm is oscillating at time $\tau = 0$ but that the amplitude of the oscillation decreases in each period. At the end, the oscillation dies in an attractor point that corresponds with $\lambda_b = 1.02$. From this value is concluded that the final state of the aneurysm is a deformed non-oscillating one and that the aneurysm does not undergo any bifurcation.

3.3. Viscous CSF and Pulsatile Blood Pressure

Finally, we introduce an internal pulsatile pressure. We perform the calculations for $\kappa = 0.05$ since it is the value for which the aneurysm's oscillation experiments some attenuation. So finally, figure 4 shows the phase diagram corresponding to the outer surface of the aneurysm, being the dashed line the transient response of the aneurysm whereas the solid red one, the steady state. The transient response corresponds with a gradual reduction in the velocity and amplitude of the oscillations until it reaches the steady state, where the motion of the oscillations becomes periodic and follows a limit cycle. The limit cycle appears because of the balance between the work resulting from the applied pressure and the energy dissipated due to the parameter κ and corresponds with the cycle in the phase diagram around which the oscillation of the wall of the aneurysm stabilizes.
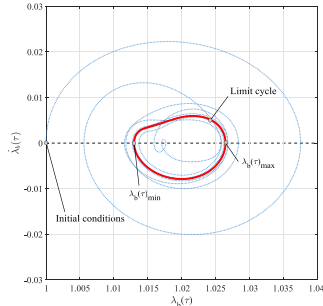

Figure 4: *Phase diagram showing the effect of a variable internal pressure in the aneurysm's model at $\overline{\rho} = 0.9524$, $f_0 = 0.7806$, $\kappa = 0.05$ and $\overline{\omega} = 1$ for the Neo-Hookean model.*

4. Conclusions

Along this work we have develop a 3D mathematical model that describes the dynamic behaviour of an idealized saccular aneurysm that has been tested for different situations and constitutive models. We have appreciated that the dynamic behaviour of mathematical model is highly influenced by the constitutive model employed; just a precise energy-function fitted for biological parameters will return a correct behaviour of the aneurysm. Moreover, we have seen that pressure and thickness seems to affect the rupture of the aneurysm's wall and that some value of $\kappa \sim 0.05$ will collaborate in the attenuation of the oscillation. Finally, it has been observed that when we introduce into the model an internal pulsatile pressure, the aneurysm reaches a limit cycle and oscillates constantly in time.

References

[1] Tortora, G. J., and Derrickson, B. Principles of Anatomy & Physiology, 13th ed. John Wiley & Sons, 2012.

[2] Chalouhi, N., Hoh, B. L., and Hasan, D. Review of cerebral aneurysm formation, growth and rupture. *Journal of the American Heart Association*, vol 40, 2013, pp 3613-3622.

[3] Meng, H., Tutino, V., Xiang, J., and Siddiqui, A. High wss or low wss? complex interactions of hemodynamics with intracranial aneurysm initiation, growth, and rupture: Toward a unifying hypothesis. *American Journal of Neuroradiology*, vol 35, sup 7, 2014, pp 1254-1262.

[4] Akkas, N. Biomechanical Transport Processes. *Springer*, 1990. Chapter: Aneurysms as a biomechanical instability problem.

[5] Austin, G., Schievink, W., and Williams, R. Controlled pressure-volume factors in the enlargement of intracranial aneurysms. *Neurosurgery*, vol 24, sup 5, 1989, pp 722-730.

[6] Jain, J. Mechanism of rupture in intracranial saccular aneurysms. *Surgery*, vol 54, sup 2, 1963, pp 347-350.

[7] Sekhar, L. N., and Heros, R. C. Growth, origin and rupture of saccular aneurysms: A review. *Neurosurgery,* vol 8, sup 2, 1981, pp 248-260.

[8] Sekhar, L. N., Sclabassi, R. J., Sun, M., Blue, H. B., and Wasserman, J. F. Growth, origin and rupture of saccular aneurysms: A review. *Stroke*, vol 19, sup 3, 1988, pp 352-356.

[9] Simkins, T., and Stehbens, W. Vibrational behavior of arterial aneurysms. *Letters in Applied and Engineering Sciences*, sup 1, vol 85, 1973, pp 100.

[10] Hung, E. J., and Botwin, M. R. Mechanics of rupture of cerebral saccular aneurysms. *Journal of Biomechanics,* vol 8, sup 6, 1975, pp 385-392.

[11] Shah, A. D., and Humphrey, J. D. Finite strain elastodynamic of intracranial saccular aneurysms. *Journal of Biomechanics*, vol 32, 1999, pp 593-599.

[12] David, G., and Humphrey, J. D. Further evidence of the dynamic stability of intracranial saccular aneurysms. *Journal of Biomechanics*, vol 36, 2003, 1143-1150.

[13] Macdonald, D. J., Finlay, H. M., and Canham, P. B. Directional wall strength in saccular brain aneurysms from a polarized light microscopy. *Annals of Biomedical Engineering*, vol 28, 2000, pp 533-542.

[14] Costalat, V., Sanchez, M., Ambard, D., Thines, L., Lonjon, N., Nicoud, F., Brunel, H., Lejeune, J. P., Dufour, H., Bouillot, P., Lhaldky, J. P., Kouri, K., Segnarbieux, F., Maurage, C. A., Lobotesis, K., Villa-Uriol, M. C., Zhang, C., Frangi, A. F., G., M., Bonafé, A., Sarry, L., and Jourdan, F. Biomechanical wall properties of human intracranial aneurysms resected following surgical. *Journal of Biomechanics*, vol 44, sup 15, 2011, pp 2685-2691.

[15] Ogden, R. Non-linear Elastic Deformations. Dover Civil and Mechanical Engineering. *Dover Publications*, 1997.

[16] Ferguson, G. G. Direct measurement of mean and pulsatile blood pressure at operation in human intracranial saccular aneurysms. *Journal of Neurosurgery*, vol 36, sup 5, 1972, pp 560-563.

[17] Ramón Lozano, Clara, Non-linear vibrations of an idealized saccular aneurysm. *E-archivo Universidad Carlos III de Madrid,* 2017.

[18] Williams, B., Poulter, N., Brown, M., Davis, M., McInnes, G., Potter, J., Sever, P., and Thom, S. M. Guidelines for management of hypertension: report of the fourth working party of the british hypertension society, *Journal of Human Hypertension*, vol 18, 2004, pp 139-185.

[19] Isaksen, J. G., Bazilevs, Y., Kvamsdal, T., Zhang, Y., Kaspersen, J. H., Waterloo, K., Romner, B., and Ingebrigtsen, T. Determination of wall tension in cerebral artery aneurysms by numerical simulation. *Stroke*, vol 39, 2008, pp 3172-3178.